ChemComm

Accepted Manuscript

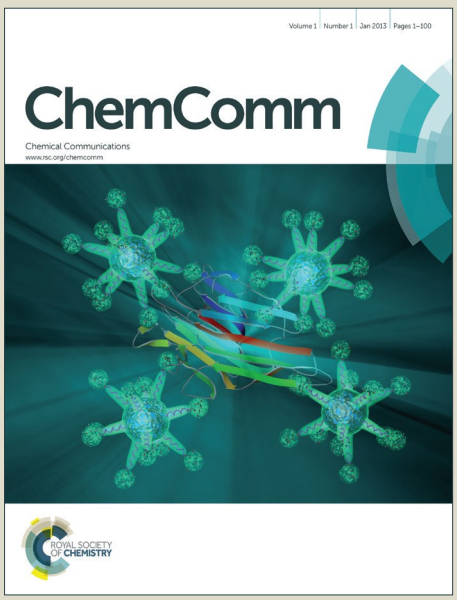

ROYAL SOCIETY OF CHEMISTRY

www.rsc.org/chemcomm

ChemComm

COMMUNICATION

Single molecule study of initial structural features on the amyloidosis process

Received 00th January 20xx,
Accepted 00th January 20xx

DOI: 10.1039/x0xx00000x

www.rsc.org/

Yong-Xu Hu,[a] Yi-Lun Ying,[a]* Zhen Gu,[a] Chan Cao,[a] Bing-Yong Yan,[b] Hui-Feng Wang,[b] and Yi-Tao Long[a]*

We employed α-hemolysin (α-HL) nanopore as single-molecule tool to investigate the effects of initial structure on the amyloidosis process. The initial structure difference of two β-amyloid (Aβ) peptides (Aβ25-35 and Aβ35-25) could be real-time distinguished due to their characteristic blockades. More importantly, the distinct aggregate dynamics for these two kinds of Aβ fragments can be readily analyzed by monitoring the blockade frequecy over time.

Introduction

Alzheimer disease (AD) is associated with the pathological self-assembly of β-amyloid (Aβ) peptide into toxic soluble oligomers and then into insoluble fibrils. Typically, an Aβ peptide is excessively formed in AD brains by processing of the amyloid precursor protein (APP).[1-4] The origin of Aβ aggregation is essential for developing an understanding of the pathologic process of amyloidosis. Previous studies demonstrate that monomeric intermediate of Aβ can affect aggregation kinetic behaviour that follows.[5] However, the correlation between initial structural differences of single monomeric Aβ and the assembly process of individual Aβ peptide over time remains to be explored. The traditional methods such as circular dichroism spectrum[6] and UV spectroscopy[7] could only provide information about the bulk solution rather than the individual features. Electron microscopy[8, 9] techniques provide the clear information on the structure of Aβ aggregates in solid-state, which are incapable of studying morphological changes in aqueous solution. Therefore, it currently exists a critical need to interpret the initial structural effects of a monomeric Aβ peptide on the dynamic behaviours of an individual Aβ aggregates in aqueous solution.

Nanopore technique provides a powerful tool to explore the single-molecule properties of peptides in aqueous solution without destroying the morphology of the analytes.[10-13] By applying a transmembrane potential, a single peptide is driven through a nanopore, which produces the transient changes in ionic current. The analysis of duration, current amplitude as well as the occurrence of each blockade reveal the characteristics of an individual peptide.[14-16] The previous attempts in nanopores have emerged to reveal the progressive changes of Aβ peptides in the view of their structures or sizes. For example, a lipid-coated solid-state nanopore was fabricated to characterize the size distribution of Aβ1-40 oligomers.[17] A protein nanopore demonstrated the potential for investigating the interactions between β-amyloid peptide fragment Aβ16-22 with various metals.[18, 19] A previous work in our group used α-hemolysin (α-HL) protein pore to probe the aggregation transition of Aβ1-42 induced by Congo red or inhibited by β-cyclodextrin.[20] In this work, we used an α-HL pore to monitor the initial structure features on the time-dependent aggregation process of two β-amyloid peptide fragment, Aβ25-35 and Aβ35-25, which possess the different structure resulted from different charged states of terminal residues. Aβ25-35 is a fibril-forming peptide (sequence GSNKGAIIGLM), containing functional domain of full-length β-amyloid peptides to forming β-sheet structure. It maintains the biologically active and toxic form of the full-length Aβ monomer.[2] The reversible-sequence Aβ35-25 which prefers random coil structure could abolishes the oxidative stress and neurotoxic properties.[22] Herein, the initial structural difference of Aβ25-35 and Aβ35-25 was real-time characterized by an α-HL nanopore (Fig. 1). The structures of random coil and β-sheet for a single monomeric Aβ exhibit two characteristic blockades, respectively. Nanopore monitoring of the following self-aggregate process clearly demonstrated that Aβ25-35 aggregates quickly whereas Aβ35-25 maintains their monomeric structure in the solution.

[a] Key Laboratory for Advanced Materials & Department of Chemistry, East China University of Science and Technology, Shanghai 200237, P. R. China
[b] School of Information Science and Engineering, East China University of Science and Technology, Shanghai 200237, P. R. China
†E-mail: yilunying@ecust.edu.cn, ytlong@ecust.edu.cn.
Electronic Supplementary Information (ESI) available: [The results for nanopore studies]. See DOI: 10.1039/x0xx00000x

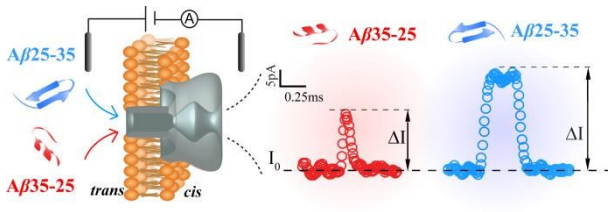

Fig. 1 Illustration of Aβ35-25 and Aβ25-35 traversing through the α-HL pore. Aβ35-25 and Aβ25-35 adopt random coil (red) and β-sheet (blue) as their initial structures, respectively. Their initial structures could be real-time distinguished by their characteristic blockades. A biological α-HL nanopore was embedded in a lipid bilayer. The two compartments of the bilayer cell are termed as *cis* and *trans*. The *cis* compartment was defined as the virtual ground. The potential was applied using a pair of Ag/AgCl electrodes. The current traces were recorded in solutions containing 1.0 M KCl, 10 mM Tris, and 1 mM EDTA buffer (pH = 8.0) at – 60 mV.

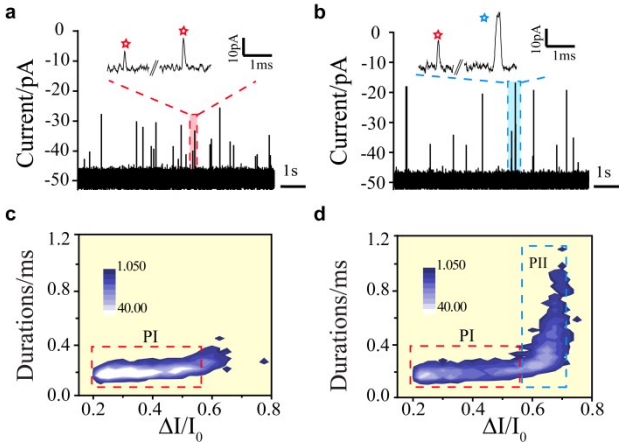

Fig. 2 Representative current traces of (a) Aβ35-25 and (b) Aβ25-35. 2D contour plots of (c) Aβ35-25 and (d) Aβ25-35. The majority of blockades for Aβ35-25 are located in I/I_0 < 0.57. The blockades of Aβ25-35 are classified into two populations as PI and PII. The population ranging from I/I_0 of 0.57 to 0.70 was defined as PII, whereas the population of I/I_0 < 0.57 was appointed to PI. The range of PII is determined by the width of a Gaussian peak (see Fig. S1). The peptides were added from the *trans* chamber containing 1.0 M KCl at an applied potential of -60 mV. The concentrations of the analyte were kept at 500 μM. The stars indicate the capture of random coil (red) and β-sheet (blue) of Aβ peptides.

Results and discussion

The mushroom-shaped α-HL consists of a cap domain termed as *cis* side and a β-barrel facing the *trans* side with diameter of approximated 20 Å along the lumen region.[23] Here, The freshly prepared peptides were driven towards the *trans* side of the lumen to promote the interactions between peptides and the lumen of the pore (Fig. 1). The current traces of Aβ35-25 and Aβ25-25 are shown in Fig. 2a-b. The 2D contour plots display that the majority of the events for monomeric Aβ35-25 is concentrated on the population I (PI) with a low current amplitude and a short duration time (Fig. 2c). In contrast, Aβ25-35 produces characteristic distributions labelled as PII with a high current amplitude at a centre of $\Delta I/I_0$ = 0.63 ± 0.02 (Fig. 2d and Fig. S1). Here, ΔI is defined as the blockage current amplitude produced by the analyte and I_0 as the open pore current. Voltage-dependent studies of Aβ fragments show that both the interval time (τ_{ON}) and blockade durations (τ_{OFF}) of Aβ35-25 decrease with the increasing negative potential (Fig. 3a-b). As a previous study suggested that the frequency of bumping events decrease with the applied potential.[24] Therefore, the collisions of Aβ35-25 towards the *trans* opening of the pore have little contribution to PI. Associated with the low amplitude of PI events and voltage-dependent increase of τ_{OFF}, we attribute PI events of Aβ35-25 mainly to the translocation events of random-coil structure through the α-HL from its *trans* side in aqueous solution.[18]

Since Aβ25-35 generated two populations as PI and PII (Fig. 2d), we further analysed the intervals and durations for each population in detail. As shown in Fig. 3c, the intervals for PI (τ_{ON-I}) and PII (τ_{ON-II}) decrease with increasing negative potential. Similar to Aβ35-25, the duration time corresponding to PI (τ_{OFF-I}) of Aβ25-35 generates positive voltage dependence (Fig. S2). The circular dichroism spectra revealed that Aβ25-35 contains both random coil and β-sheet structure in aqueous solution.[25] Therefore, the PI events of Aβ25-35 is mainly ascribed to the translocation of random coil form of Aβ25-35 through the α-HL. However, the duration time of PII (τ_{OFF-II}) increases with the negative applied potentials (> - 60 mV), and reaches a minimal value at -60 mV (Fig. 3d). Since the lacking of a peptide-pore interaction originates a monotonically decreasing function of durations with the potential, the non-monotonically voltage-dependent change of τ_{OFF-II} suggests that the peptide strongly interact with the α-HL protein pore before translocating through *cis* side or exiting from *trans* side.[24] The X-ray diffraction measurements of Aβ25-35 give rise to a 4.5 ± 0.1 Å distance between two neighbouring chains of a β-sheet secondary structures and a 10.6 Å distance between side chains of β-sheet structure.[26] Because the average diameter of lumen for α-HL is approximate 20 Å,[23] β-sheet structure of Aβ25-35 could undergoes strong interactions with the pore lumen before exiting from either the *trans* or *cis* opening, inducing a volume exclusion of the ionic current. By recognizing the characteristic blockades, the β-sheet structure of Aβ25-35 could be well distinguished with α-HL pore in real time (Fig. 2b). As shown in Fig. 3c, the PI events of Aβ25-35 exhibit higher probability at a less negative potential (- 40 mV and - 60mV) compared with PII events. As the potential shifts to more negative ones (<-60mV), the occurrence of PII events is higher than that of PI events. This may be resulted from the decrease of bumping events in PI with increasing negative potential.[24] The structure difference between Aβ35-25 and Aβ25-35 suggest that the structure in Aβ monomer mainly results from the distribution of charged residues. In Aβ25-35, the interactions between positive side chain of the K28 and the negative C-terminus make it capable to form β-hairpin conformation.[27]

In order to study the initial structural effects of Aβ25-35 and Aβ35-25 on the self-aggregation tendency, we compared event frequencies of Aβ25-35 and Aβ35-25 with incubation time period of 84 h, respectively. As shown in Fig. 4a-b, the frequency of both PI and PII blockades for Aβ25-35 displays a strong time-

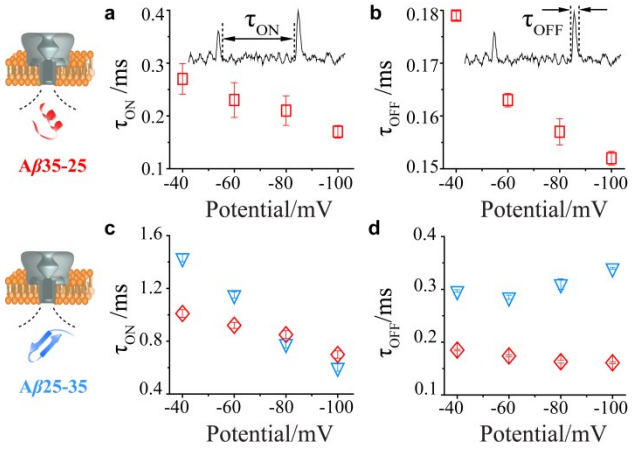

Fig. 3 Voltage dependence of τ_{ON} (a) and τ_{OFF} (b) for the freshly prepared Aβ35-25 peptide. The effect of voltage on the value of τ_{ON} (c) and τ_{OFF} (d) for the PI (red) and PII (blue) blockades of the freshly prepared Aβ25-35. Fig. S2 displays the plots of voltage-dependent duration for Aβ35-25 and Aβ25-35 in the same scale. The values of τ_{ON} were carried out by the single-exponential fittings and τ_{OFF} were fitted by Gaussian function (see Fig. S3). A large value of τ_{ON} suggests that the blockades occur at a low frequency and vice versa. Data of the errors were based on three separate experiments. The concentration of the analyte were kept at 500 μM.

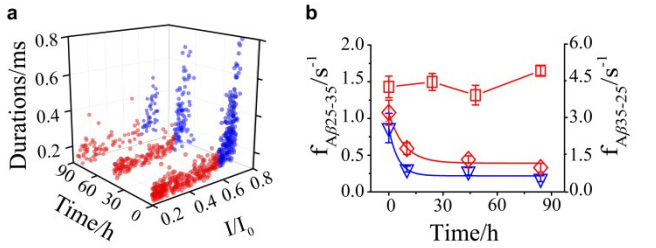

Fig. 4 (a) Scatter plots of Aβ25-35 blockades within 5 mins recording for the incubation time of 0 h, 44 h and 84 h, respectively. (b) Frequency of blockades for Aβ25-35 (PI in red diamond and PII in blue triangle) and Aβ35-25 (red square) versus incubation time. The frequency-time curve of Aβ25-35 were fitted into a single-exponential function $f = A + B*exp(-kt)$. Data of the errors were based on three separate experiments. The peptides were added from the *trans* chamber containing 1.0 M Tris-KCl at an applied potential of -60 mV.

dependent decrease. Moreover, our studies demonstrate that the blockade frequency of β-sheet structure is proportional to the increasing concentration of freshly prepared Aβ25-35 (Fig. S4). Therefore, the transformation of initial structures of Aβ25-35 into larger aggregates produced a decrease of event frequency with the incubation time. The scatter plots of Aβ25-35 solutions that had been permitted to aggregate for various hours show that there are no new distributions of blockades comparing with freshly prepared sample (Fig. 4a). These results indicate that the large aggregates are hardly driven to the *trans* opening of the α-HL pore at applied potential due to the less charge exposed in larger Aβ aggregates.[28] In general, the amyloidosis process follows a sigmoidal curve including initial lag phase, fast exponential growth and a plateau.[29] The aggregation rate k can be extracted by fitting a single exponential to the growth phase.[30] In order to obtain the aggregation rate in our nanopore experiments, the frequency-time curve of β-sheet structure were fitted into a single-exponential function, giving the k of 5.45 $\times$ 10^{-5} s^{-1}. In addition, a rapid decrease for the frequency of β-sheet structure in Aβ25-35 is accompanied by a fall in the frequency of random coil. However, the event frequency of random coil structure in Aβ35-25 remains relative constant with the incubation time (Fig. 4b). A previous study by CD spectrum demonstrates that random coil structure has a tendency to transform into β-sheet structure in the aggregate process.[6] Therefore, we could speculate that the random coil structure in Aβ25-35 undergoes structure conversion to form β-sheet structured fibrils. Similarly to Aβ25-35, there were no new distributions of Aβ35-25 occurring along with incubation time (Fig. S5). These results reveal that Aβ35-25 with random coil structure is reluctant to aggregate in a long incubated time, which in agreement with non-neurotoxicity of this peptide.[22] On the basis of previous hypothesis for aggregate mechanism, fibrils Aβ molecules are organized in antiparallel β-sheets structure, which formed by residues 31–34 and 28–30 of vicinal peptide and the interactions between the hydrophobic side chains of two other monomers.[27] The β-sheet structures are considered as the "seeds" to prompt Aβ monomers to aggregate into soluble oligomer, then into insoluble β-amyloid plaque.[31] The MD simulation shows β-sheet structures exist as intermediate in early aggregate and their stability is associated with aggregate rate.[5] This is consistent with our results that Aβ25-35 is prone to forming β-sheet structure and promotes aggregate process followed.

Conclusions

In summary, we employed α-HL as a single-molecule tool to real-time investigate self-assembly property of two β-amyloid peptide fragments, Aβ25-35 and Aβ35-25, which possess the different initial structures. Our study obtains two characteristic blockades which are assigned to random coil and β-sheet of Aβ fragments, respectively. Further analysis of the event frequency shows the distinct aggregate kinetics for these two Aβ fragments. Our research sheds light on the initial structural effects of Aβ peptide on its conformational transition from monomeric amyloid β-peptide into large aggregates, which would benefit the understanding of the amyloidosis in AD.

Acknowledgements

This work was supported by the National Natural Science Foundation of China (21327807 and 21505043). Y.-L. Ying is supported by the 57rd Chinese Post-doctor Fund (2015M570336).

Notes and references

1 J. Nunan and D. H. Small, *FEBS Lett.,* 2000, **483**, 6-10.
2 Y. G. Kaminsky, M. W. Marlatt, M. A. Smith and E. A. Kosenko, *Exp. Neurol*. 2010, **221**, 26-37.

3 J. P. Cleary, D. M. Walsh, J. J. Hofmeister, G. M. Shankar, M. A. Kuskowski, D. J. Selkoe and K. H. Ashe, *Nat. Neurosci*., 2005, **8**, 79-84.
4 L. Millucci, L. Ghezzi, G. Bernardini and A. Santucci, Curr. *Protein Pept. Sci*., 2010, **11**, 54-67.
5 B. Ma and R. Nussinov, *Biophys. J*., 2006, **90**, 3365-3374.
6 M. Naldi, J. Fiori, M. Pistolozzi, A. F. Drake, C. Bertucci, R. Wu, K. Mlynarczyk, S. Filipek, A. De Simone and V. Andrisano, *ACS Chem. Neurosci*., 2012, **3**, 952-962.
7 L. Millucci, R. Raggiaschi, D. Franceschini, G. Terstappen and A. Santucci, *J. Biosci*., 2009, **34**, 293-303.
8 C. Giordano, A. Sansone, A. Masi, A. Masci, L. Mosca, R. Chiaraluce, A. Pasquo and V. Consalvi, *Chem. Biol. Drug Des*., 2012, **79**, 30-37.
9 A. J. Nicoll, S. Panico, D. B. Freir, D. Wright, C. Terry, E. Risse, C. E. Herron, T. O'Malley, J. D. Wadsworth and M. A. Farrow, *Nat. Commun*., 2013, **4,** 1-9.
10 A. Oukhaled, L. Bacri, M. Pastoriza-Gallego, J.-M. Betton and J. Pelta, *ACS Chem. Biol*., 2012, **7**, 1935-1949.
11 Y.-L. Ying, C. Cao and Y.-T. Long, *Analyst*, 2014, **139**, 3826-3835.
12 J. E. Reiner, A. Balijepalli, J. W. Robertson, J. Campbell, J. Suehle and J. J. Kasianowicz, *Chem. Rev.*, 2012, **112**, 6431-6451.
13 L.-Q. Gu and J. W. Shim, *Analyst*, 2010, **135**, 441-451.
14 H.-Y. Wang, Z. Gu, C. Cao, J. Wang and Y.-T. Long, *Anal. Chem*., 2013, **85**, 8254-8261.
15 T. C. Sutherland, Y.-T. Long, R.-I. Stefureac, I. Bediako-Amoa, H.-B. Kraatz and J. S. Lee, *Nano Lett*., 2004, **4**, 1273-1277.
16 Y.-L. Ying, D.-W. Li, Y. Liu, S. K. Dey, H.-B. Kraatz and Y.-T. Long, *Chem. Commun*., 2012, **48**, 8784-8786.
17 E. C. Yusko, P. Prangkio, D. Sept, R. C. Rollings, J. Li and M. Mayer, *ACS nano*, 2012, **6**, 5909-5919.
18 A. Asandei, I. Schiopu, S. Iftemi, L. Mereuta and T. Luchian, *Langmuir*, 2013, **29**, 15634-15642.
19 A. Asandei, S. Iftemi, L. Mereuta, I. Schiopu and T. Luchian, *J. Membrane. Biol*., 2014, **247**, 523-530.
20 H.-Y. Wang, Y.-L. Ying, Y. Li, H.-B. Kraatz and Y.-T. Long, *Anal. Chem*., 2011, **83**, 1746-1752.
21 T. Kubo, S. Nishimura, Y. Kumagae and I. Kaneko, *J. Neurosci. Res*., 2002, **70**, 474-483.
22 G. Olivieri, G. Baysang, F. Meier, F. Müller‐Spahn, H. Stähelin, M. Brockhaus and C. Brack, *J. Neurochem*., 2001, **76**, 224-233.
23 L. Song, M. R. Hobaugh, C. Shustak, S. Cheley, H. Bayley and J. E. Gouaux, *Science*, 1996, **274**, 1859-1865.
24 L. Movileanu, J. P. Schmittschmitt, J. M. Scholtz and H. Bayley, *Biophys. J*., 2005, **89**, 1030-1045.
25 G. Wei and J.-E. Shea, *Biophys. J*., 2006, **91**, 1638-1647.
26 D. A. Kirschner, H. Inouye, L. K. Duffy, A. Sinclair, M. Lind and D. J. Selkoe, *Proc. Natl. Acad. Sci*., 1987, **84**, 6953-6957.
27 L. Larini and J.-E. Shea, *Biophys. J.*, 2012, **103**, 576-586.
28 M. Kittner and V. Knecht, *J. Phys. Chem.: B*, 2010, **114**, 15288-15295.
29 F. S. Ruggeri, J. Adamcik, J. S. Jeong, H. A. Lashuel, R. Mezzenga and G. Dietler, *Angew. Chem.-Int. Edit*, 2015, **54**, 2462-2466.
30 F. Chiti, N. Taddei, F. Baroni, C. Capanni, M. Stefani, G. Ramponi and C. M. Dobson, *Nat. Struct. Mol. Biol.*, 2002, **9**, 137-143.
31 P. S.-W. Yeung and P. H. Axelsen, *J. Am. Chem. Soc*., 2012, **134**, 6061-6063.